JOURNAL OF GEOPHYSICAL RESEARCH, VOL. 93, NO. B9, PAGES 10,489–10,500, SEPTEMBER 10, 1988

Evidence for a Sharp 670-km Discontinuity as Inferred From *P*-to-*S* Converted Waves

HANNEKE PAULSSEN

Department of Theoretical Geophysics, Institute of Earth Sciences, Utrecht, The Netherlands

The fine structure of the upper mantle discontinuities is investigated using observations of converted waves on short-period and broadband seismograms. Using a stacking technique to analyze the *P* wave coda of teleseismic records, evidence is found for coherent near-receiver *P*-to-*S* converted phases generated by the 400- and 670-km discontinuity beneath a number of the stations used in this study. Variations in travel time, slowness, and amplitude of these phases as observed among the stacks for stations of the Regional Seismic Test Network in the United States and of the Network of Autonomously Recording Seismographs in western Europe are very likely the expression of upper mantle heterogeneity. Observations of coherent converted phases from the 400-km discontinuity are fewer in number than of phases converted at the 670-km discontinuity, suggesting that the latter is more pronounced. Some of the seismograms, especially of station RSCP, show extremely high-amplitude *P*-to-*S* converted phases from the 670-km discontinuity. These seismograms allow a detailed waveform comparison of the converted phase with the direct *P* phase and present evidence for a sharp 670-km discontinuity.

INTRODUCTION

Nearly all upper mantle velocity models published in the last two decades show two discontinuities at depths of about 400 and 670 km. They mark the upper and lower boundary of the transition zone and are called the 400- and 670-km discontinuity, respectively, although their actual depths may differ from these two values. In spite of the large amount of studies on the upper mantle velocity structure, there is still no general consensus about the nature of these two discontinuities. They can be related to phase transformations in olivine-rich mineral assemblages as well as to chemical transitions [cf. *Jeanloz and Thompson*, 1983; *Anderson and Bass*, 1986]. Accurate seismological data are required to constrain petrological models of the upper mantle and the nature of the discontinuities. The depth resolution of the seismic velocity structure at the discontinuities, based on upper mantle refracted waves, appears insufficient to distinguish between a phase transformation and a change in chemical composition. Detailed information on the sharpness of the discontinuities, an important parameter to discriminate between the two alternatives, can be obtained from upper mantle reflected and converted waves. These waves sample the discontinuities locally with relatively short wavelengths. A serious drawback is that these phases are generally of low amplitude, which hampers their identification.

In this study the upper mantle discontinuities are investigated with near-station *P*-to-*S* converted waves from teleseismic events. These phases arrive in the coda of the direct *P* wave and have the polarization of teleseismic *SV* waves. Since the arrival time of these waves is much less than those of the direct *S* wave, we can conclude that any *SV*-polarized wave in this coda must have been converted from *P*. Thus, contrary to other waves that have been studied such as *S*-to-*P* conversions, or underside reflections like *P'670P'*, their identification is not in doubt. The location of conversion can be estimated by the time delay with respect to the *P* phase.

Paper number 7B5087.
0148-0227/88/007B-5087$05.00

The signal-to-noise ratio of the low amplitude phases is increased by stacking the data of different events for a single station, which enhances the near-receiver effects and allows an estimate of the coherence of the signal. It is shown that coherent energy, originating from the upper mantle beneath the station, arrives in the time interval of 40–80 s after the *P* phase. Arrivals with an *SV* polarization and a delay and slowness consistent with an interpretation of a *P*-to-*S* converted wave from the 670-km discontinuity (*P670s* phase), can be identified for several of the stations used in this study. These include the five short-period Regional Seismic Test Network (RSTN) stations in the United States, the short-period Seismic Research Observatory (SRO) station CHTO in Thailand, and five of the broadband stations of the Network of Autonomously Recording Seismographs (NARS) in Europe. The results of the short-period stations not only confirm the results of previous studies [*Vinnik*, 1977; *Kosarev et al.*, 1984; *Paulssen*, 1985] but also complement these with high-frequency information, presenting evidence for an extremely sharp 670-km discontinuity beneath one of the RSTN stations. The *P670s* arrivals observed for the stations of the NARS array are more complicated in nature, which may reflect a complex nature of the 670-km transition or a high degree of lateral heterogeneity beneath the stations. Upper mantle *P*-to-*S* converted waves from the 400-km discontinuity (*P400s*) are less consistently observed, and the data of this study suggest that this transition is less sharp or of smaller velocity contrast than the 670-km discontinuity.

DATA SELECTION AND METHOD OF ANALYSIS

The data which have been used for this study are obtained from Global Digital Seismograph Network (GDSN) event tapes covering the period January 1985 to May 1986, and from NARS event tapes of the interval January 1983 to April 1987. The data have been selected according to the following criteria:

1. Only short-period (SP) and broadband (BB) data are considered. Long-period seismograms are discarded because of the inherent limitations in attainable resolution.

2. No primary phases must arrive in the time interval of interest. This interval starts at about 40 s after the direct *P* wave when the amplitude of the crustal phases is negligible. To avoid interference with phases such as *PP* and *PcP*, only teleseismic

events are analyzed ($65° < \Delta < 90°$), and to prevent interference with *pP* and *sP* arrivals, only shallow (<80 km) and deep (>400 km) events have been used.

3. The available length of the seismograms must extend to at least 80 s after the *P* arrival to allow a possible identification of *P*-to-*S* converted phases from the 670-km discontinuity (*P670s*).

4. The data quality, as checked by visual inspection, must display a high signal-to noise ratio and a clear *P* onset.

Furthermore, the number of seismograms per station must be sufficient to guarantee a reliable interpretation of the receiver effects of the *P* wave coda. This is the case for the SP data of the five RSTN stations and SRO station CHTO (Thailand) with 15–47 seismograms per station, as well as for five of the BB NARS stations with 17–48 seismograms per station (stations NE04, NE05, NE06, NE15, and NE16).

To allow an unambiguous interpretation of the near-receiver phases, the data have been stacked. The stacking technique is essentially a τ-Δp stack, where τ in this case is the differential time with respect to the *P* phase and Δp the slowness difference with the direct *P* wave. The three components (vertical, radial, and transverse) of each seismogram are cross-correlated with the waveform of the *P* phase on the vertical. The data are then normalized with respect to the autocorrelation of the *P* phase to give each seismogram equal weight. After that, the data are stacked using reference values for τ and Δp appropriate for a *P* wave arriving at an epicentral distance of 72° for the data of the RSTN stations and station CHTO and at 80° for the NARS data. These two values are approximately the mean values of the distribution of epicentral distances per station and yield an optimum slowness resolution. The mean and standard deviation σ of the stack (as a function of time) are calculated to obtain an estimate of the coherence in the stacked signal. Assuming a Gaussian distribution, the 95% confidence level of the signal (mean $\pm$ 2σ) can then be determined, allowing for an easy interpretation of the statistical significance of the stacked data. As an example, the τ-Δp diagram of the radial component of station RSCP with an indication of the 95% confidence interval (reflected in the width of the trace) is shown in Figure 1. Similar diagrams have been used to analyze the vertical, radial, and transverse component of the *P* wave coda of all the stations.

Phases are "identified" for which the mean stacked amplitude is larger than twice the standard deviation at that time. In this respect, it is important to know that the standard deviation of the SP and BB stacks generally is 1.5–3% of the amplitude of the *P* phase on the vertical in the 40- to 80-s interval. Arrivals with an amplitude smaller than about 3–6% of the direct *P* wave are therefore not expected to be resolved using the 95% confidence criterion. Phases have been interpreted as *P*-to-*S* conversions when "arrivals" on the radial component are not in phase with the signal on the vertical component, i.e., do not have a longitudinal polarization.

The technique, modified from *Vinnik* [1977], thus enhances all signals, on each of the three components, that are similar to the chosen waveform, and may therefore be used to investigate all phases that correlate strongly with the *P* pulse. In most cases, the *P* pulse has been defined by the first "sinelike" waveform, usually about 2–3 s long. The method was found to be quite robust with respect to the selected signal under the condition that its duration is not too long (about 5–6 s). This is probably due to the fact that crustal phases then contaminate the *P* waveform. The technique is in this respect different to the one often used to study the crustal structure beneath a station [e.g., *Phinney*, 1964; *Langston*, 1979; *Owens et al.*, 1987]. In this (latter) method, "receiver functions" for steeply incident *P* waves are obtained by the deconvolution of the radial component by the vertical component. It is then implicitly assumed that the vertical component contains the direct arrival (including source effects) but also most of the unwanted receiver crustal reverberations. The receiver function is therefore most sensitive to crustal *P*-to-*S* converted phases, whereas reverberations are suppressed. This is an adequate technique for determining the crustal structure, but it is less satisfactory for the identification of (deep) upper mantle converted phases because the upper mantle *P*-to-*S* converted phases are not affected in the same way by the crustal structure as the direct *P* wave. Hence crustal multiples should preferably not be included in the "source term" as they degrade the deconvolution for the upper mantle converted phase. Using the technique described above, crustal multiples are enhanced instead of suppressed because of their similarity with the *P* pulse. This explains the large amplitude of the "ringing" after the first *P* arrival as seen in Figure 1 for $\Delta p = 0$ km/s. (This information could be useful to constrain the crustal *P* wave velocity structure; receiver functions are more sensitive to the *S* wave velocity structure.)

OBSERVATIONS OF *P*-TO-*S* CONVERTED WAVES FROM THE 670-KM DISCONTINUITY

Several "arrivals" of coherent energy can be recognized on the stack of Figure 1, but most interesting is the wavelet at τ=68 s, Δp=-0.0025 s/km which is the only prominent arrival with the character of a near-vertical incident *SV* wave in the time interval of interest (see Figure 2*a*). The phase at 63 s for a differential slowness of -0.035 s/km is clearly not an *SV* arrival (see Figure 2*c*), whereas the phase at 71 s for the same differential slowness might be interpreted as a *P*-to-*S* conversion, although its polarization is more consistent with that of a *P* wave. The signal at τ = 68 s and Δp = -0.0025 s/km has a duration equal to that of the stacked *P* phase (at Δp=0 s/km), and its amplitude is 15% of that of the *P* wave on the vertical. To investigate the significance of the phase in more detail, the data set of this station is divided into two sets with different back azimuth. Although more noisy, both subsets show the same *SV* arrival (see Figure 2*b*), indicating that there is no (or little) azimuthal dependence of the signal.

Timing, amplitude, and polarization eliminate the possibility of a crustal origin of the phase. Furthermore, the arrival has a slowness smaller than that of the direct *P* wave, making an explanation as a crustal multiple more unlikely, as multiples have larger slownesses than the direct phase in a radially symmetric Earth. The polarization (near-vertical incident *SV*), and timing (coda of *P* wave) can only be explained by a phase converted from *P* to *SV* in the upper mantle beneath the station.

Reference Earth models such as 1066B [*Gilbert and Dziewonski*, 1975] and PREM [*Dziewonski and Anderson*, 1981] predict a delay of 68–69 s for a *P*-to-*S* conversion from the 670-km discontinuity, suggesting that the phase is generated by the 670-km discontinuity. Its theoretical slowness is approximately 0.0013 s/km smaller than that of the *P* phase according to these models, a value slightly lower than estimated from the τ-Δp stack, but the arrival clearly has a negative differential slowness, as is predicted for a *P*-to-*S* converted phase. The reference models do not explain the extremely high amplitude (15% of direct *P* wave on the vertical) of the *P670s* phase as observed on the stack of station RSCP. Calculated by the WKBJ method (for perfectly elastic, radially symmetric media), PREM predicts an amplitude of 5.2% of that of the *P* phase. Model 1066B, with a relatively high velocity (10%) and density (7%) contrast across the 670-km

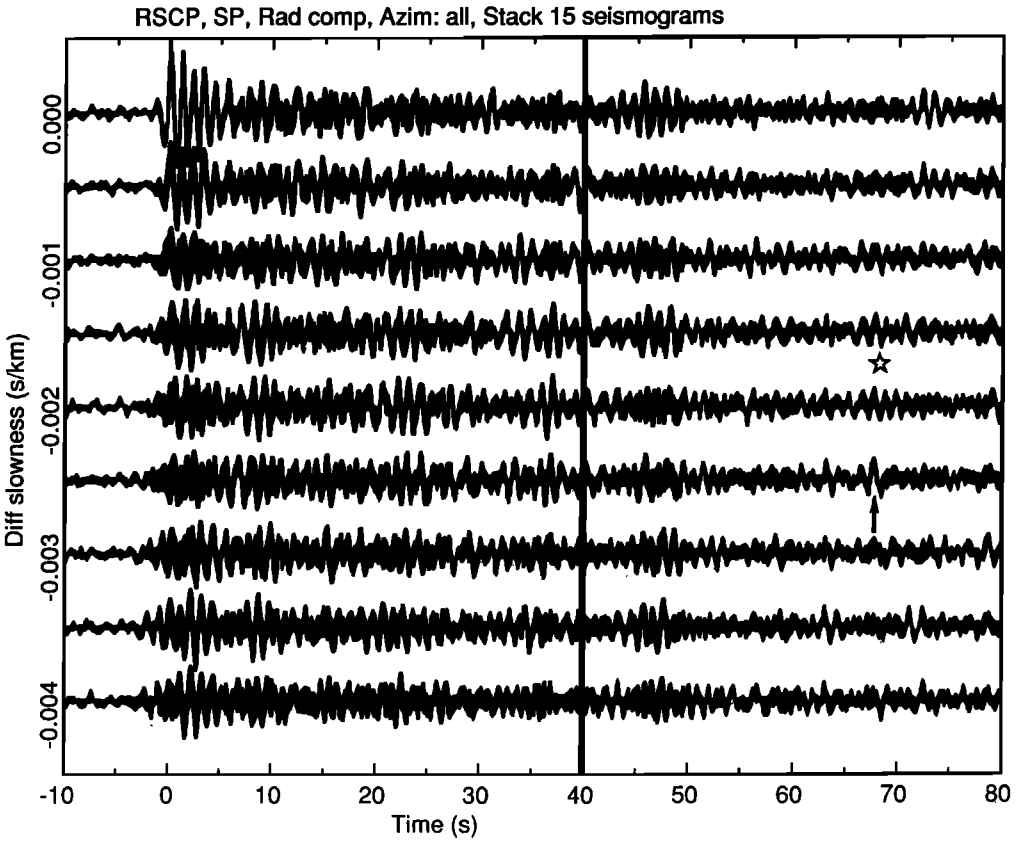

Fig. 1. The τ-p - stack of the radial component of the (correlated and normalized) seismograms of station RSCP (for an epicentral distance of 72°). Indicated by the width of the trace is the mean ±2 times the standard deviation (95% confidence interval) for each differential slowness relative to that of the direct P wave. The arrow points to a clear SV- arrival, and the star indicates the theoretical arrival of the $P670s$ phase according to model 1066B. No primary phases arrive in the interval between 40 and 80 s, the beginning of which is marked by the vertical line.

discontinuity (see *Nolet and Wortel* [1988] for an overview of upper mantle velocity models), gives an amplitude of 8.7% of that of the P phase. Obviously, the cause of the observed high amplitude must, at least partially, be sought in the structure beneath the station.

Conjectures that local effects contribute to a strong $P670s$ phase at RSCP (Cumberland Plateau, Tennessee) are confirmed by inspection of the individual seismograms. Figure 3 shows examples of seismograms with arrivals identified as $P670s$. Enlargements of the relevant portions of the data of Figures 3*b*–3*d* can be found in Figures 4*a*–4*c*. The amplitudes of the phases on the (SP or BB) radial component reach values as high as 45–65% of that of the P phase on the vertical but are, except for the example of Figure 3*a*, still at about noise level which makes them difficult to identify. A notable feature of these seismograms is that the energy on the radial component is generally nearly as high as that on the vertical, even for the teleseismic P waves. The cause of this high-amplitude signal on the radial component is not yet evident, but it might be related to location of the station on a sedimentary layer (see *Owens et al.* [1984] for the crustal structure beneath RSCP; this model predicts a radial/vertical amplitude ratio of about 25% for a teleseismic P wave with Δ = 72°, which is clearly not consistent with the observations). *Bouchon and Aki* [1977] modeled the response of a sedimentary basin to a local earthquake for wavelengths which are close to the dimension of the geological structure, and a strong amplification of the horizontal motions is their main result. Although the cause of the high amplitudes on the radial component is not yet fully understood, it is evident that the amplitudes of the P-to-S converted phases at RSCP may not simply be interpreted as an effect of the 670-km transition.

Another noteworthy feature of the high-amplitude $P670s$ phases is the similarity between the waveforms of the converted and the nonconverted waves as shown in Figures 4*a*–4*c*. The resemblance of the P and $P670s$ waveforms is striking, given the noise level of the data (judged by the differences in the vertical and radial component for the P phase). The similarity between the P and $P670s$ phase is also made clear by comparison of the amplitude spectra of the phases of Figure 3*c* (seen in Figure 4*d*). The wavelet of the converted phase resembles that of the direct P phase at least up to frequencies of 2 Hz (station noise dominates at higher frequencies).

The SP data of the other RSTN stations and station CHTO were analyzed in detail to investigate whether the $P670s$ phase could also be observed for these stations. However, the stacked seismograms of these stations did not yield equally evident results. There is some evidence for the presence of a $P670s$ phase on the stacks of the stations RSON (Red Lake, Ontario), RSNT (Yellowknife, Northwest Territory), and RSSD (Black Hills, South Dakota), where the signal is just statistically significant within the 95% confidence level (see Figures 5*a*–5*c*). At τ = 70, 72, and 69 s the amplitudes of the stacked signal are 4.3, 4.5, and 5.0% of that of the P phase for RSON, RSNT, and RSSD, respectively, values that are in accordance with a PREM velocity

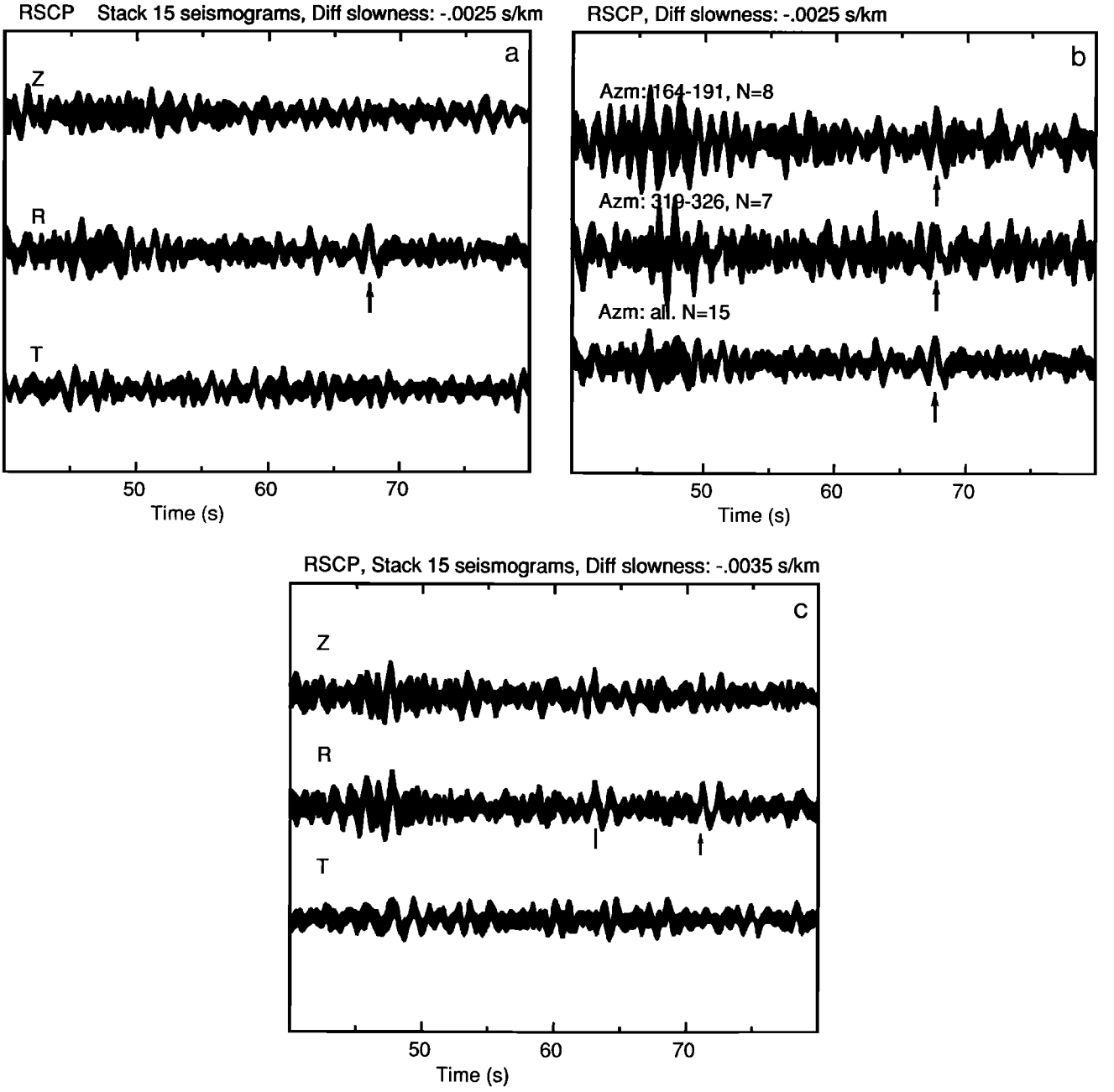

Fig. 2. (*a*) The 95% confidence interval of the stacked (correlated and normalized) seismograms of the vertical (*Z*), radial (*R*), and transverse (*T*) component of station RSCP for a differential slowness of -0.0025 s/km. (*b*) The 95% confidence levels of the radial component of the stacked seismograms of station RSCP with a back azimuth of 164°–191° (upper trace, eight seismograms), with a back azimuth of 319°–326° (middle trace, seven seismograms), and of total data set (lower trace). (*c*) The 95% confidence interval of the stacked (correlated and normalized) seismograms of the vertical (*Z*), radial (*R*), and transverse (*T*) component of station RSCP for a differential slowness of -0.0035 s/km.

contrast at 670 km. The interpretation of the data at RSSD is complicated by coherent signals on the vertical component just before and after the possible *P*670*s* arrival. Note also that there are high-amplitude arrivals on the transverse component of this station, which is probably due to the pronounced lateral variations in the crustal structure beneath this station [*Owens et al.*, 1987]. There is no conclusive evidence for the presence of a *P*-to-*S* converted phase from the 670-km discontinuity on the stacked seismograms of station RSNY (Adirondacks, New York) and CHTO (Chiang Mai, Thailand), as can be seen from Figures 5*d*–5*e*.

Similar to the SP data, the BB data of the NARS array give varying results regarding possible *P*670*s* arrivals. Figure 6*a* shows the 95% confidence interval of the radial component of the stacks of the five NARS stations of this study. The arrows point to wavelets with an *SV* polarization, and two more or less consistent arrivals can be recognized: one at 66 s and one at 72 s.

The stacked seismograms of station NE15 (Valkenburg, The Netherlands) show a clear *SV* arrival at $\tau = 66$ s, with an estimated slowness of $\Delta p = -0.0010$ s/km, and an amplitude which is 7.3% of the amplitude of the direct *P* phase on the vertical with a standard deviation of 2.4% (7.3 ± 2.4%, this notation will be used

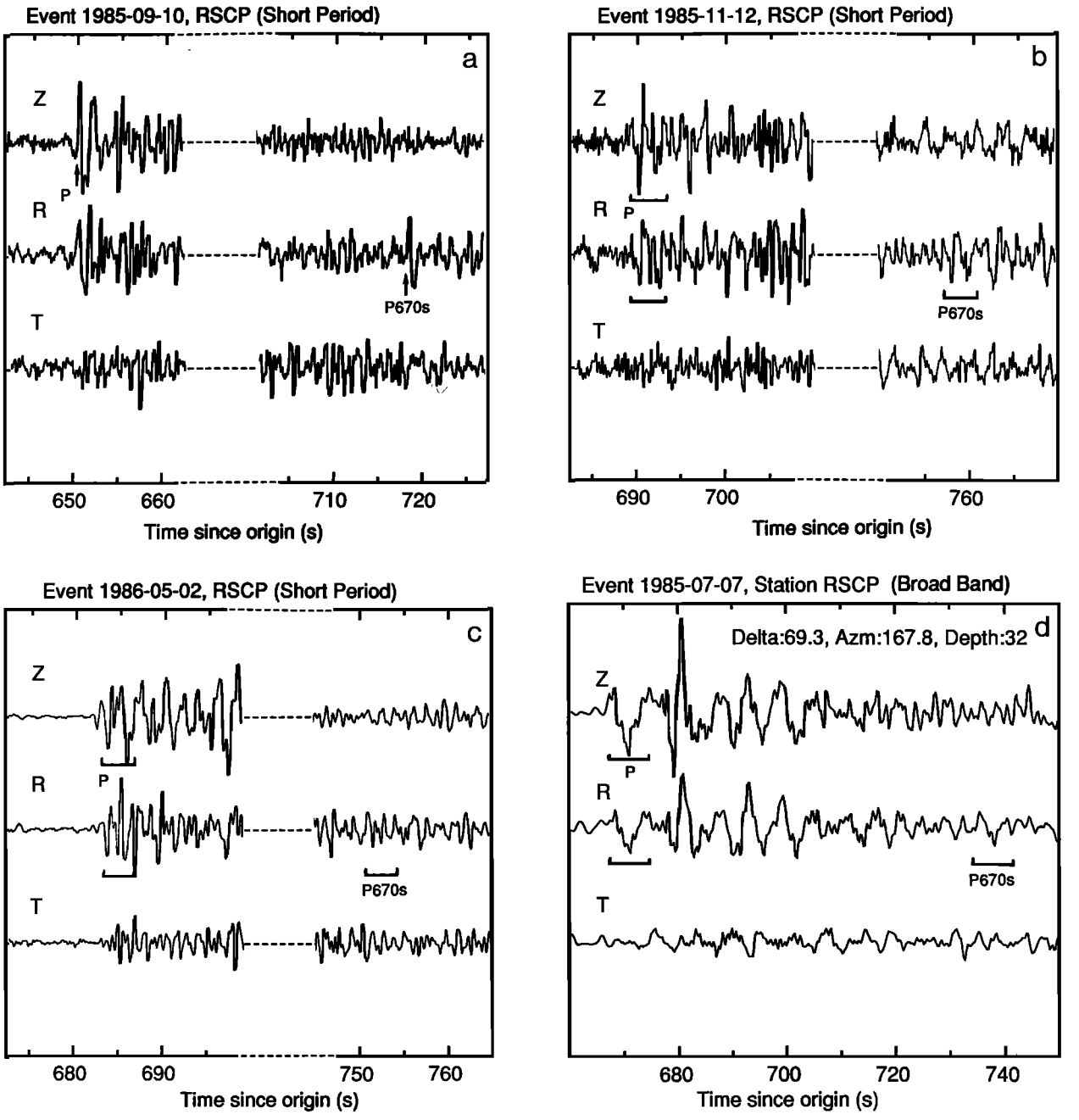

Fig. 3. Vertical (Z), radial (R), and transverse (T) component of the SP seismograms of stations RSCP of event (*a*) 1985-09-10: depth 33 km, back azimuth 329°, delta 66.8°; (*b*) 1985-11-12: depth 10 km, back azimuth 191°, delta 72.4°; (*c*) 1986-05-02: depth 33 km, back azimuth 325°, delta 89.9°; and (*d*) of the BB seismogram of event 1985-07-07: depth 32 km, back azimuth 167.8°, delta 69.3°.

in the following). The phase has a duration equal to that of the stacked P phase and is observed on different substacks of the data. It therefore seems to be a coherent phase, but it is difficult to identify on the individual seismograms. Apparently, the phase is generally not of high amplitude, except perhaps for the one shown in Figure 7*a* with a delay of 65 s. The other two stations in The Netherlands (NE04 Witteveen and NE05 Utrecht) and station NE06 (Dourbes, Belgium) show at best poorly resolved SV waves at 66 s with amplitudes of about 5.0 ± 2.3%. Examination of subsets of the data reveals that the arrival at 66 s is not consistently observed at NE04 and NE05 (see also *Paulssen* [1985]) but, although with smaller amplitude, appears more coherent at NE06. Figure 7 shows examples of seismograms with phases that are identified as P-to-S conversions for different NARS stations with a delay of approximately 66 s.

The most coherent signal with an SV character observed for station NE16 (Clermont Ferrand, France) is at the arrival at 72 s (Δp = -0.0010 s/km, amplitude = 8.7 ± 2.7%). However, the phase is not recognized on any of the individual seismograms due to the generally high amplitude ("noisy") coda of the data. A similar remark could be made concerning the arrival at 73 s for station NE04, although the "coda noise" is of this station is smaller in amplitude. The wavelet at 70–76 s observed for station NE06 is a feature of seismograms with a northeast back azimuth

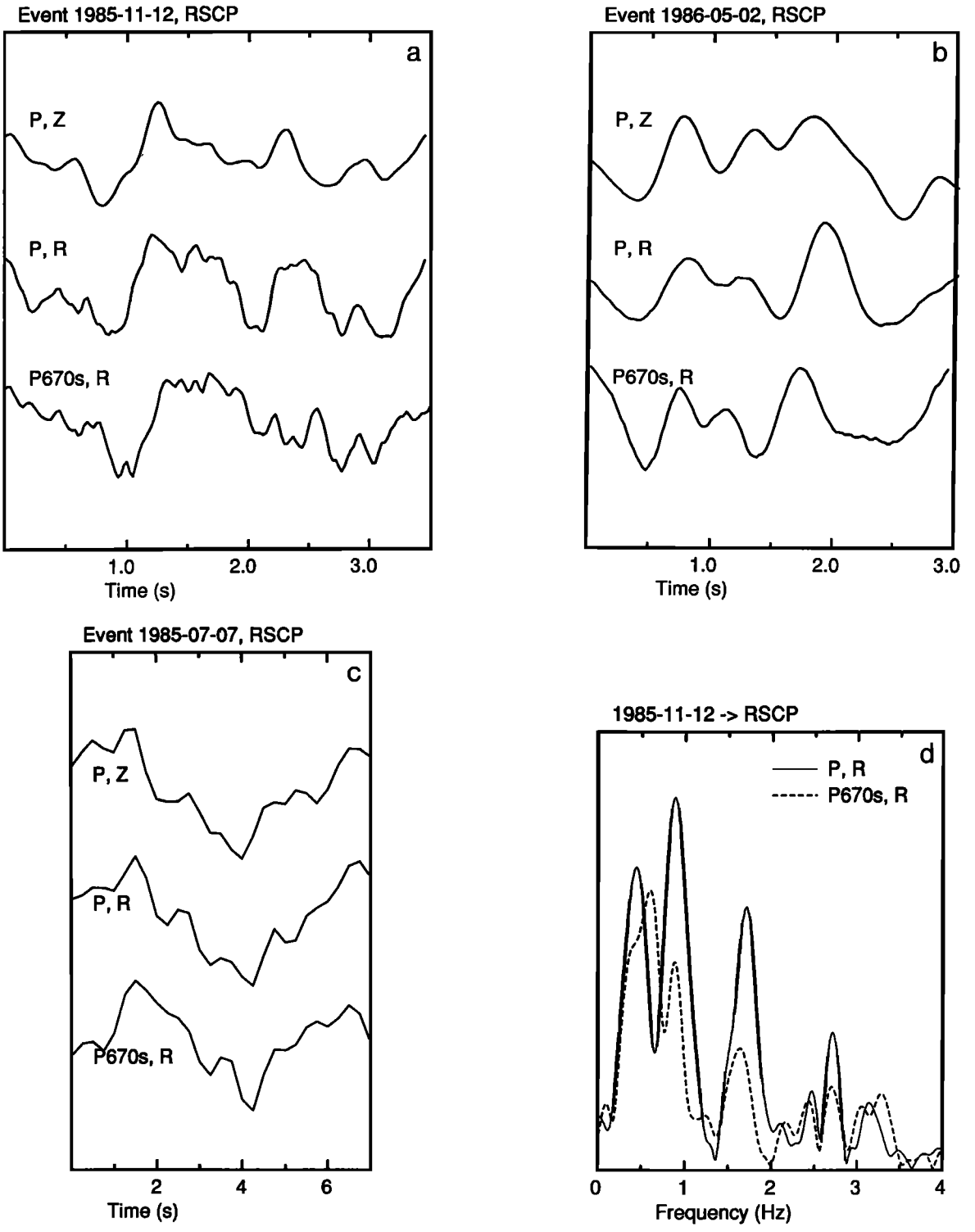

Fig. 4. Waveforms of the direct *P* phase on the vertical and radial component (upper and middle trace) and of the *P670s* phase on the radial component (lower trace) of (*a*) event 1985-11-12 (cf. Figure 3*b*), (*b*) event 1986-05-02 (cf. Figure 3*c*), (*c*) event 1985-07-07 (cf. Figure 3*d*), and (*d*) frequency content of the *P* waveform on radial component (solid curve) and of the *P670s* phase on the radial (dashed curve) of event 1985-11-12. (Vertical scale is linear.)

only. Although some of the seismograms of these stations show a high-amplitude signal on the radial component at about 72–74 s after the *P* arrival, these cannot unambiguously be interpreted as upper mantle converted phases.

Another interesting feature, shown in Figure 6*b*, is a very clear *SV* arrival at 80 s in the coda of NE04 for data with a back azimuth of about 345°–41° (Δp = 0 s/km, amplitude = 11.4 ± 3.1%), and a similar but less clear phase for NE05 (Δp = 0 s/km, amplitude = 10.1 ± 4.6%) for which the available seismograms have a predominantly northeast back azimuth. The phase is not observed for any of the other stations and is recognized on the seismograms of NE04 and NE05 by an increase in amplitude.

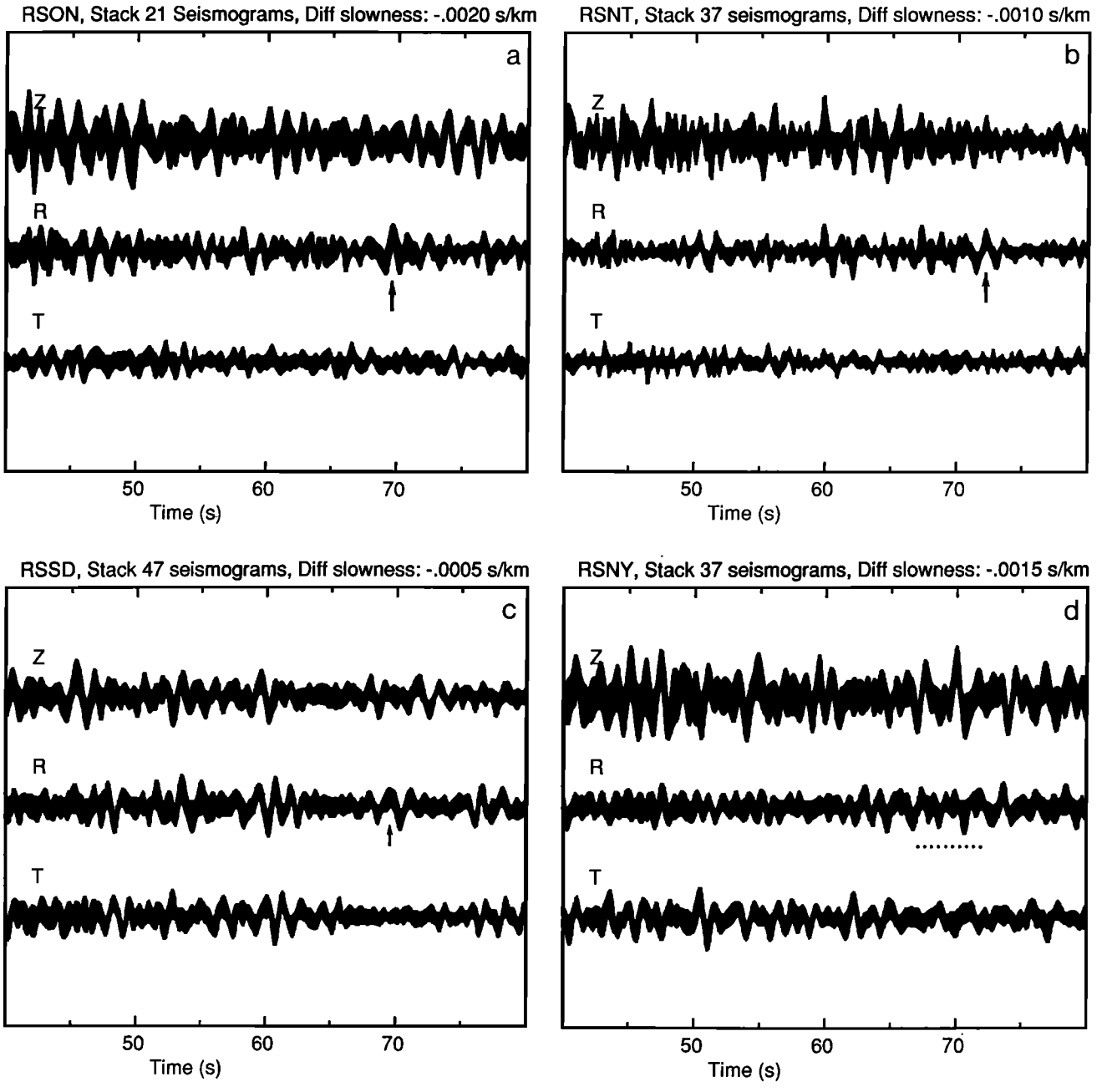

Fig. 5. Stacked (correlated and normalized) seismograms of the vertical (*Z*), radial (*R*), and transverse (*T*) component of the stations (*a*) RSON, (*b*) RSNT, (*c*) RSSD, (*d*) RSNY, (*e*) CHTO. The number of seismograms and differential slowness used for these stacks are indicated at the top of each diagram.

Waveform comparisons with the direct *P* are not as convincing as for phases arriving at approximately 66 s, the phase generally being recognized by an increase of energy on the radial component. This, together with the estimated differential slowness of 0.0 s/km and the limited number of stations and azimuthal range for which these observations are made, hampers the interpretation as simple upper mantle *P*-to-*S* converted waves.

OBSERVATIONS OF *P*-TO-*S* CONVERTED PHASES FROM THE 400-KM DISCONTINUITY

The observations of the *P670s* phase stimulated a detailed investigation into the presence of other converted phases from the upper mantle. Although there is some evidence for the existence of other *SV* arrivals in the time window of 40–80 s after the *P* phase, none of these phases is very systematically observed. Most coherent and clear are the phases with a delay of 43–49 s. Two RSTN stations show an *SV* arrival at 48–49 s after the *P* phase (RSNY: τ = 48 s, Δp = -0.0005 s/km, amplitude = 5.0 ± 1.3%; RSNT: τ = 49 s, Δp = -0.0020 s/km, amplitude = 4.5 ± 1.2%), and three NARS stations show an *SV* phase with a delay of 44–46 s (NE04: τ = 44 s, Δp = -0.0040 s/km, amplitude = 6.3 ± 1.9%; NE06: τ = 46 s, Δp = -0.0025 s/km, amplitude = 2.8 ± 1.4%; NE16: τ = 44 s, Δp = -0.0005 s/km, amplitude = 9.0 ± 2.7%). Figure 8 shows the 95% confidence intervals of the radial component of these data. If these phases are interpreted as *P*-to-*S* converted phases from the upper mantle they must be related to the 400-km discontinuity. Model PREM and 1066B predict

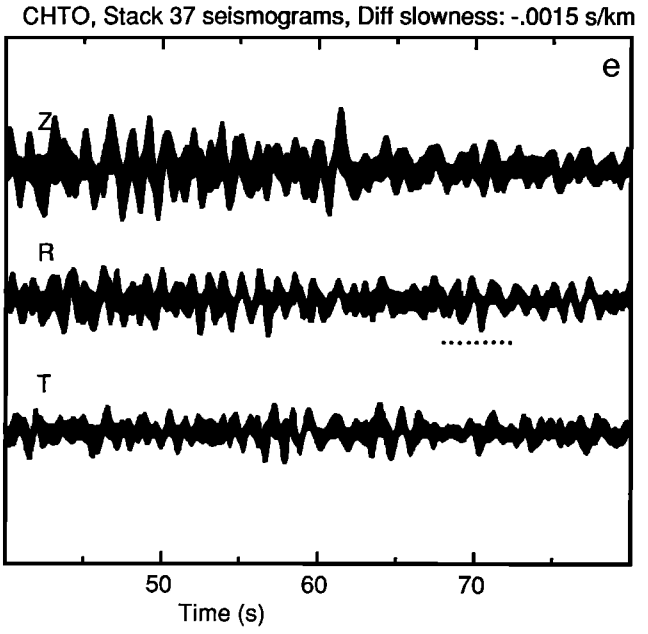

Fig. 5. (continued)

delays of 42 and 44 s for discontinuities at depths of 400 and 420 km, respectively, and delays of 43 and 46 s if a more acceptable continental crust is incorporated. The differential slowness is -0.0007 s/km according to PREM and -0.0005 s/km for 1066B, and theoretical amplitudes are approximately 2.5% of the *P* wave. The amplitudes of the *P*400*s* phases are smaller than those of *P*670*s* phases, mainly because of a smaller velocity contrast in the two reference models at the 400-km discontinuity. Observations of *P*400*s* phases are indeed smaller in number than those of *P*670*s* phases, but the stacked amplitudes range from 2.8 to 9.0%, values that are comparable to those of *P*670*s* phases. These variations in estimated amplitude, travel time, and slowness point to lateral heterogeneity at or above the 400-km discontinuity. No clear *P*400*s* phases have been identified on individual seismograms, which could imply that there are no high-amplitude *P*400*s* phases or that there is more waveform distortion than for the *P*670*s* phases. More data are needed to solve this question and to allow an interpretation in terms of the width and velocity contrast of the discontinuity.

INTERPRETATION

It is shown that the stacked seismograms may allow an identification of the upper mantle *P*-to-*S* converted phases beneath the seismic station if the signal-to-noise ratio is sufficiently reduced by stacking. The amplitude estimates as obtained from the stacks should be interpreted as lower bounds of the "true" mean amplitudes, since small travel time differences due to crustal and upper mantle heterogeneity beneath the station will reduce the amplitude of the stacked signal, especially for the SP data. Furthermore, it should be kept in mind that the inferred differential slownesses are only estimates of which the resolution depends on the distribution of epicentral distances. The visually estimated "slowness resolution" of the τ-Δp stacks is for all stations approximately 0.0005 s/km, except for RSON (± -0.0010 s/km).

The results of this study show clear *P*-to-*S* converted phases from the 670-km discontinuity for the SP data of station RSCP (τ = 68 s, amplitude = 13.7 ± 3.6%, Δp = -0.0025 s/km) and for the BB data of stations NE15 (τ = 66 s, amplitude = 7.3 ± 2.4%, Δp = -0.0010 s/km) and NE16 (τ = 72 s, amplitude = 8.7 ± 2.7%, Δp = -0.0010 s/km).

Less clear are the *P*670*s* phases on the SP stacks of RSON (τ = 70 s, amplitude = 4.3 ± 1.7%, Δp = -0.0020 s/km), RSNT (τ = 72 s, amplitude = 4.5 ± 2.1%, Δp = -0.0010 s/km), RSSD (τ = 69 s, amplitude = 5.1 ± 2.5%, Δp = -0.0005 s/km), and possibly the phase at RSCP (τ = 71 s, amplitude = 11.0 ± 4.9%, Δp = -0.0035 s/km). The other BB NARS stations present a series of signals with an *SV* wave character between 66 and 76 s. These signals are just statistically significant within the 95% confidence limit, but it is difficult to trace their origin. The arrivals can be interpreted as conversions from interfaces at different depths, but they can also be explained by lateral heterogeneity beneath the station, resulting in variations of the arrival times for phases generated by the 670-km discontinuity. The data of station NE06 seem to point in this direction as the wavelet between 70 and 76 s is a feature of data with a northeast back azimuth only. However, most clear *P*670*s* arrivals have been identified on seismograms of different NARS stations in northwest Europe with a delay of 66 ± 2 s, and this arrival is more or less consistently observed on the stacks of these stations (NE04, NE05, NE15, and NE06) for different azimuths. The question of whether the later arrivals are due to different interfaces or to lateral heterogeneity cannot be resolved with this data set. The intermittent nature of observations of *P*-to-*S* converted phases from the 670-km discontinuity is further inferred

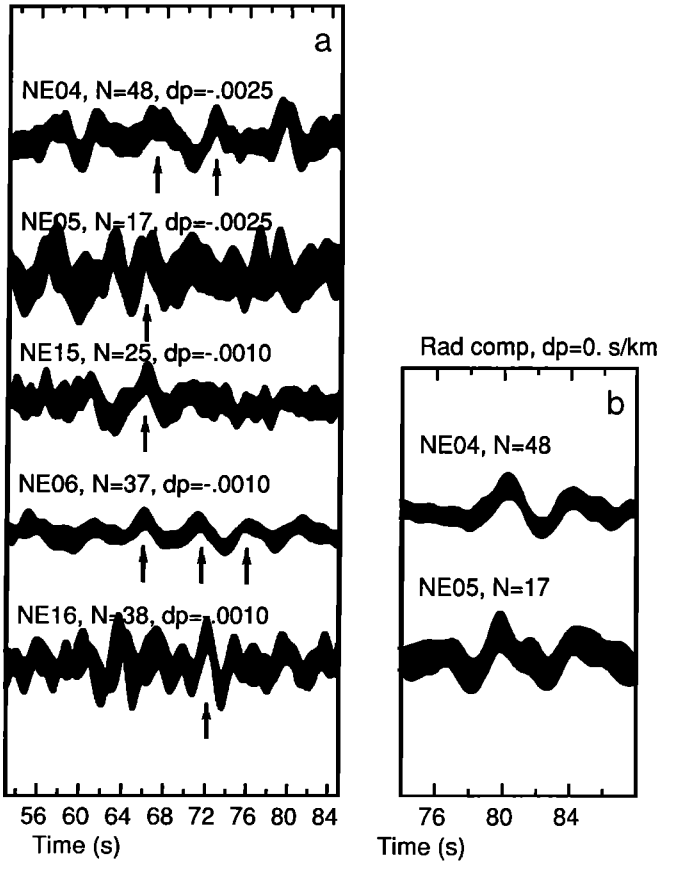

Fig. 6. (*a*) The 95% confidence intervals of the stacked signal on radial component for the NARS stations of this study. Station name, number of seismograms used for the stack, and differential slowness are indicated at the top of each trace. Arrows point to arrivals with an *SV* polarization. (*b*) The 95% confidence intervals of the stacked signal on the radial component for station NE04 and NE05 for Δp = 0.0 s/km.

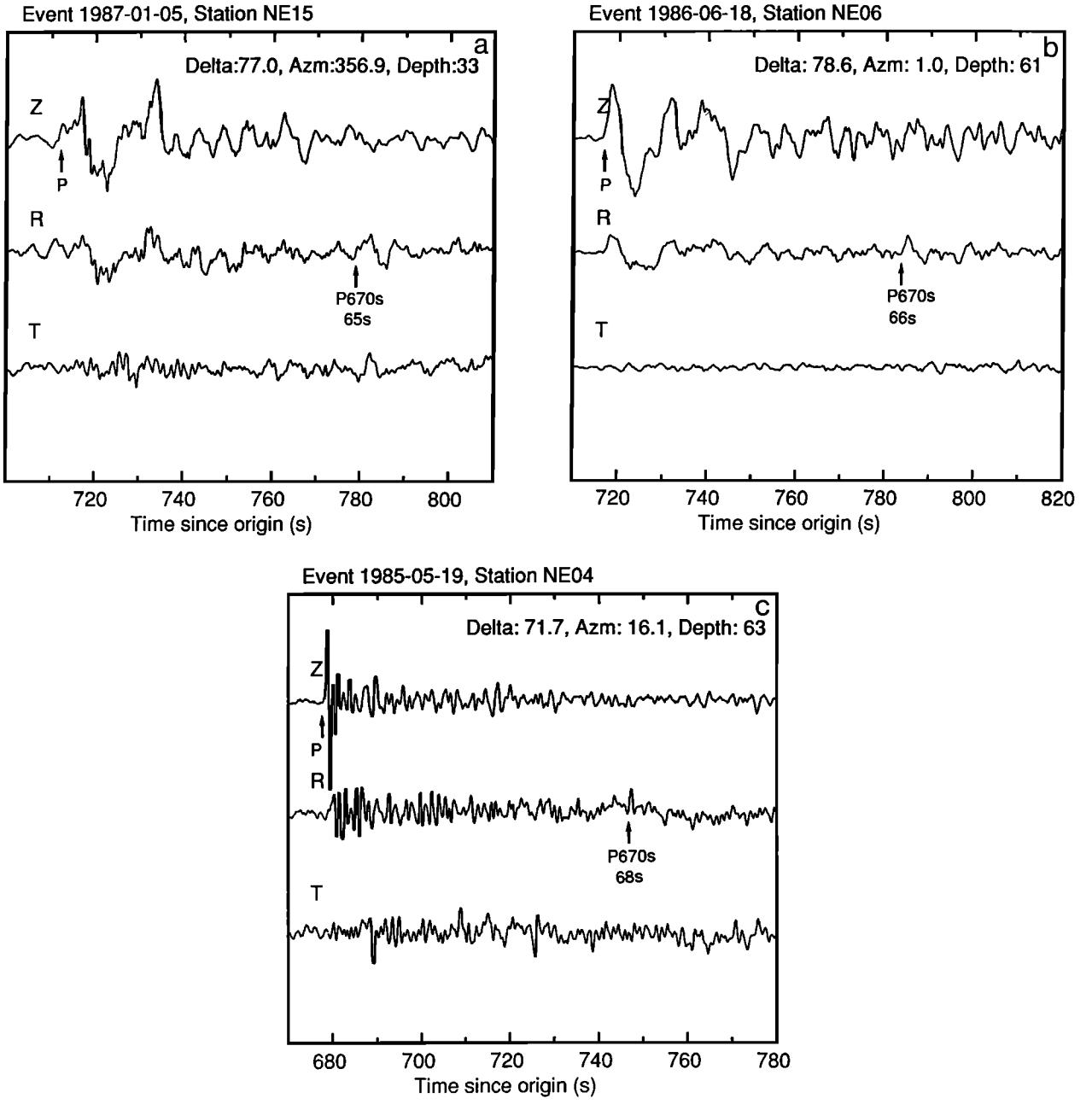

Fig. 7. Examples of *P670s* phases for different NARS stations in northwest Europe.

from the SP stacks of station RSNY ($\sigma \approx 1.3\%$) and CHTO ($\sigma \approx 1.9\%$) which do not show any evidence for the presence of such a phase.

The identified *P670s* phases on the SP and BB seismograms of station RSCP and on the BB seismograms of NARS stations show extremely high amplitudes that cannot be explained by acceptable radially symmetric upper mantle models. It is believed that the high amplitudes are at least partly due to the local structure beneath the station. Supporting this view is the observation that clear *P670s* phases on individual seismograms are predominantly identified for stations located on sediments, which might imply that focusing effects of the sediment-basement interface play an important role. However, high-amplitude *P670s* phases can also result from focusing effects of other structures in the crust or upper mantle. In particular, focusing by warping of the 670-km discontinuity is very effective due to its large impedance contrast for *P*-to-*S* converted waves (see also *Paulssen* [1985]). The travel time and slowness variations as observed for the *P670s* phases are further suggestive for topography of the 670-km discontinuity, although effects of upper mantle heterogeneity may not be neglected. Since a large degree of upper mantle lateral heterogeneity is likely to be present for different regions (particularly for western Europe [*Spakman et al.*, 1988; *Paulssen*, 1987]), it is not appropriate to interpret the observed travel times, slownesses, and amplitudes in a more quantitative way than the simple estimates made by *Paulssen* [1985].

More important for an interpretation of the nature of the 670-km discontinuity is the waveform similarity of the converted phases to the direct *P* wave. The waveforms of the converted phases resemble those of the *P* wave signal up to 1 Hz for the BB

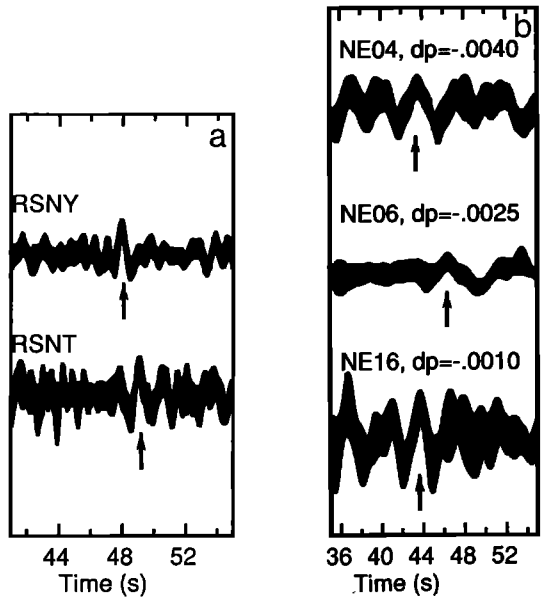

Fig. 8. (*a*) The 95% confidence intervals of the stacked signal on the radial component of SP stations RSNY (N = 37, Δp = -0.0005 s/km), and RSNT (N = 37, Δp = -0.020 s/km), and (*b*) of the BB stations NE04, NE06, and NE16. Arrows point to arrivals with an *SV* polarization.

data of Figures 3*d* and 7 and for the SP data in one particular case even up to 2 Hz (Figure 4*d*). This implies that the 670-km discontinuity is, at least locally, extremely sharp. The transfer functions shown in Figure 9 display the frequency-dependent amplitude behavior of converted phases for different widths of the discontinuity. They are calculated by the propagator matrix method for a "linear gradient" within the transition which is approximated by a sequence of layers of 1 km each. Assuming that the high-frequency content has decayed by 40 to 50% relative to the low frequencies, it can be inferred that the width of the transition must be less than 5 to 6 km for waveform "similarity" up to 1 Hz, or less than 2.5 to 3 km for waveform similarity up to 2 Hz. This observation has important implications for petrological and geodynamical models of the mantle (see discussion).

Observations of *P*-to-*S* converted waves from the 400-km discontinuity on the stacked seismograms are smaller in number, and no clear *P400s* phases have been identified on individual seismograms. This may indicate that there are no high-amplitude *P400s* phases or that there is more waveform distortion for the *P400s* phases than for the *P670s* phases. This last interpretation could imply that the 400-km discontinuity is less sharp than the 670-km discontinuity. However, to produce an amplitude of 4–5% of the *P* wave on a stack of short-period data, the 400-km discontinuity must be both sufficiently sharp ($\lesssim$ 10 km) and define a reasonable velocity contrast (>5% if no focusing effects are included).

DISCUSSION

The most important result of this study is the evidence for a locally sharp 670-km discontinuity from identifications of *P670s* phases on seismograms. A sharp 670-km transition has previously been suggested from observations of precursors to *PKPPKP* (*P'P'*) on SP seismograms. These phases have been interpreted as underside reflections from the 670-km discontinuity, denoted by *P'670P'* [*Engdahl and Flinn*, 1969; *Whitcomb and Anderson*, 1970; *Adams*, 1971; *Bolt and Qamar*, 1972; *Teng and Tung*, 1973; *Fukao*, 1977; *Husebye et al.*, 1977, *Nakanishi*, 1986]. *Cleary* [1981] questioned this interpretation and showed that such early precursors are also adequately explained by scattering of the *PKKKP* phase at the inside of the core-mantle boundary. More recently, however, *Nakanishi* [1986] argued that slowness estimates of the *P'670P'* phases of several studies do not agree with those expected for *PKKKP* scattered phases.

The sharpness of the discontinuity has been inferred from the fact that *P'670P'* phases are observed on short-period records. *Richards* [1972] showed that for a horizontally layered medium the thickness of the transition must be less than 4 km to produce observable *P'670P'* phases on SP seismograms. However, he also pointed to the importance of (a small) curvature in the reflector on the amplitude of the *P'670P'* phase. In this regard, it is should be mentioned that *P'670P'* phases are not consistently observed [*Husebye et al.*, 1977; *Nakanishi*, 1986]. Furthermore, *P'670P'/P'P'* amplitude ratios vary among different studies [*Teng and Tung*, 1973]. These observations can easily be explained in terms of focusing and defocusing effects of the discontinuity, although variations in the *P'670P'/P'P'* amplitude ratio may also occur when one phase is nearer to a caustic than the other. In both cases it is likely that high-amplitude *P'670P'* phases are predominantly observed, resulting in an overestimate of the reflectivity at the short-period frequency band and, consequently, in an overestimate of the sharpness of the discontinuity for acceptable values of the velocity contrast.

Observations of near-source *S*-to-*P* converted waves from the 670-km discontinuity below Izu-Bonin [*Barley et al.*, 1982] and the Fiji-Tonga region [*Bock and Ha*, 1984] on SP seismograms suggest a sharp transition (<10 km) in regions of subduction zones but also indicate that regional variations exist because systematic differences in the signal duration of these converted phases are recognized.

The results of the aforementioned studies strongly suggest that the 670-km discontinuity is in several locations quite sharp, but this inference was disputed by *Muirhead* [1985]. In this respect,

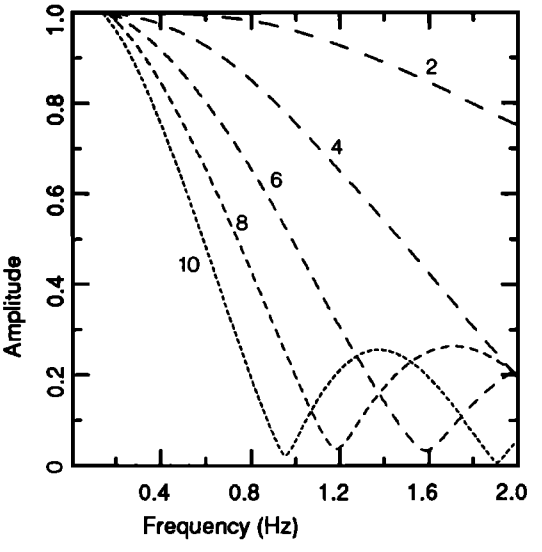

Fig. 9. Transfer functions of the frequency dependence of *P670s* phases for different widths of the 670-km discontinuity. The curves represent the (frequency dependent) amplitude ratio of phases converted at a transition of finite width to those converted at a first order discontinuity. Indicated for each curve is the width of the transition in km.

the waveform comparisons of *P* and *P*-to-*S* converted phases [*Paulssen*, 1985, 1988; this study] leave no doubt. Summarizing these results and those of other studies, generally employing LP data (*P*-to-*S* converted phases [*Vinnik*, 1977; *Kosarev et al.*, 1984; *Souriau*, 1986; *Kind and Vinnik*, 1988] and *S*-to-*P* converted phases [*Faber and Müller*, 1980, 1984; *Baumgardt and Alexander*, 1984]), it can be concluded that phases reflected or converted at the discontinuity are often, but only intermittently, observed. The number of observations and the estimated locations of reflection or conversion indicate that the discontinuity is a worldwide feature present under continents and oceans and subduction zones and ridges. There is growing evidence that the transition is locally sharp (less than 5 km) but may have regional or large-scale variations in thickness or in depth.

These seismological observations have important geodynamical implications. *Lees at al.* [1983] have shown that for plausible mantle mineralogies, models that invoke phase transitions alone produce a reflectivity in the short-period frequency band that is an order of magnitude smaller than inferred from *P'670P'*. The reflectivity for short periods critically depends on the width of the phase transformation. Using the high pressure and temperature data compiled by *Jeanloz and Thompson* [1983], Lees et al. calculate that phase transitions occur over a 10- to 40-km depth interval, depending on the mineral assemblage. These values are too high to explain the seismic observations. Recent experimental work by *Ito and Takahashi* [1987] shows that the dissociation of γ-spinel into perovskite plus magnesiowüstite, probably the most important phase transition at a depth of 650 km, is completed within a pressure interval of 1 GPa (≈ 25 km). Although this is sharp in a petrological sense (for a divariant phase transformation), the experimental data should resolve the transformation with an accuracy of less than 0.2 GPa (5 km) to be able to compare the petrological results with the seismic observations. The dissociation of majorite, a garnet solid solution, evidently cannot explain the seismic 670-km discontinuity because it occurs over a relatively wide pressure interval of about 4 GPa [*Ito and Takahashi*, 1987]. A chemical transition, or a combination of a chemical and phase transition, can easily explain the sharpness of the 670-km discontinuity (see also *Lees et al.* [1983]). A compositional change across the discontinuity would most naturally imply a chemically distinct upper and lower mantle, possibly involving two-layered convection [*Richter and Johnson*, 1974; *Christensen and Yuen*, 1984]. An alternative model is proposed by *Ringwood and Irifune* [1988]. In this model, the upper and lower mantle are assumed to be of similar bulk composition separated by a chemical boundary layer at a depth of 600–700 km, which is supposed to have formed by effects of phase changes and differentiation in subducted slabs. The phase transformation of γ-spinel to perovskite plus magnesiowustite together with the chemical change of (lenses of) former basaltic crust on top of ancient oceanic lithosphere would account for the sharp 670-km discontinuity and the variability of the (seismic) observations.

At present, it is not clear whether the upper and lower mantle are chemically distinct or not. More seismological studies are required to improve our knowledge of seismological aspects of the 670-km discontinuity to be able to answer some basic questions: Is the 670-km discontinuity only locally sharp, or is its sharpness a worldwide feature? Is topography of the 670-km discontinuity, as suggested by *Paulssen* [1985] and *Richards and Wicks* [1987], only locally significant or also on a global scale? What is the origin of the multiple *SV*-arrivals in the 66- to 72-s interval (this study)? What are the velocity and density contrasts across the discontinuity with a higher accuracy than presently known?

Short-period and broadband body wave studies of converted and reflected phases now provide the most detailed information about the sharpness and depth of the 670-km discontinuity. The results of these studies could be complemented with those of long-period (or low-passed broadband) data to investigate the frequency dependence of the variations among the observations. Upper mantle refracted phases are most adequate to determine the velocity contrast across the transition [e.g., *Walck*, 1984]. Although we are still far from "global mapping" of the upper mantle discontinuities, an increased station density combined with a sufficient quantity of broadband digital data would contribute to solve many of the ambiguities that still exist in detailed upper mantle studies.

Apart from seismological information, major advances in our understanding of the 670-km discontinuity are expected from petrological studies. These will, in the near future, resolve whether phase transformations can account for the seismic observations or not. Contributions from other fields, such as geochemical evidence, geodynamic modeling of mass transport in the mantle, information about the thermal state of the mantle, and (seismic) observations of the depth of slab penetration, will provide insight in aspects that necessary to improve our picture of the Earth's mantle and the role that the 670-km discontinuity plays in it.

Acknowledgments. I thank G. Nolet, G. Shudofsky, and N. Wajeman for their comments on a preliminary version of this paper. The NARS project was funded by AWON, the Earth Science branch of the Netherlands Organization for the Advancement of Pure Research.

REFERENCES

Adams, R. D., Reflections from discontinuities beneath Antarctica, *Bull. Seismol. Soc. Am., 61*, 1441–1451, 1971.

Anderson, D.L., and J.D. Bass, Transition region of the Earth's upper mantle, *Nature, 320*, 321–328, 1986.

Barley, B.J., J.A. Hudson, and A. Douglas, *S* to *P* scattering at the 650-km discontinuity, *Geophys. J. R. Astron. Soc., 69*, 159–172, 1982.

Baumgardt, D. R., and S.S. Alexander, Structure of the mantle beneath Montana LASA from analysis of long-period, mode-converted phases, *Bull. Seismol. Soc. Am., 74*, 1683–1702, 1984.

Bock, G., and J. Ha, Short-period *S-P* conversion in the mantle at a depth near 700 km, *Geophys. J. R. Astron. Soc., 77*, 593–615, 1984.

Bolt, B. A., and A. Qamar, Observations of pseudo-aftershocks from underground nuclear explosions, *Phys. Earth Planet. Inter., 5*, 400–402, 1972.

Bouchon, M., and K. Aki, Near-field of a seismic source in a layered medium with irregular interfaces, *Geophys. J. R. Astron. Soc., 50*, 669–684, 1977.

Christensen, U.R., and D. Yuen, The interaction of a subducting lithospheric slab with a chemical or phase boundary, *J. Geophys. Res., 89*, 4389–4402, 1984.

Cleary, J., Seismic wave scattering on underside reflection at the core-mantle boundary, *Phys. Earth Planet. Inter., 26*, 266–267, 1981.

Dziewonski, A.M., and D.L. Anderson, Preliminary reference Earth model, *Phys. Earth Planet. Inter., 25*, 297–356, 1981.

Engdahl, E.R., and E.A. Flinn, Seismic waves reflected from discontinuities within the Earth's upper mantle, *Science, 163*, 177–179, 1969.

Faber, S., and G. Müller, *Sp* phases from the transition zone between upper and lower mantle, *Bull. Seismol. Soc. Am., 70*, 487–508, 1980.

Faber, S., and G. Müller, Converted phases from the mantle transition zone observed at European stations, *J. Geophys., 54*, 183–194, 1984.

Fukao, Y., Upper mantle *P*-structure and the 650-km discontinuity, in *High Pressure Research*, edited by M.H. Manghnani and S. Akimoto, pp. 151–161, 1977.

Gilbert, F., and A.M. Dziewonski, An application of normal mode theory to the retrieval of structural parameters and source mechanisms from

seismic spectra, *Philos. Trans. R. Soc. London, Ser. A, 278*, 187–269, 1975.

Husebye, E.S., R.A. Haddon, and D.W. King, Precursors to $P'P'$ and upper mantle discontinuities, *J. Geophys., 43*, 535–543, 1977.

Ito, E., and H. Takahashi, Ultrahigh-pressure phase transformations and the constitution in the deep mantle, in *High-Pressure Research in Mineral Physics*, edited by M.H. Manghnani and Y. Syono, pp. 221–229, Terra Scientific Publishing Company, Tokyo, 1987.

Jeanloz, R., and A.B. Thompson, Phase transitions and mantle discontinuities, *Rev. Geophys., 21*, 51–74, 1983.

Kind, R., and L.P. Vinnik, The upper-mantle discontinuities underneath the GRF array from *P*-to-*S* converted phases, *J. Geophys., 62*, 138–147, 1988.

Kosarev, G.L., L.I. Makeyeva, and L.P. Vinnik, Anisotropy of the mantle inferred from observations of *P* to *S* converted waves, *Geophys. J. R. Astron. Soc., 76*, 209–220, 1977.

Langston, C.A., Structure under Mount Rainier, Washington, inferred from teleseismic body waves, *J. Geophys. Res., 84*, 4749–4762, 1979.

Lees, A.C., M.S.T. Bukowinski, and R. Jeanloz, Reflection properties of phase transitions and compositional change models of the 670-km discontinuity, *J. Geophys. Res., 88*, 8145–8159, 1983.

Muirhead, K., Comments on "Reflection properties of phase transition and compositional change models of the 670-km discontinuity" by Alison C. Lees, M.S.T. Bukowinski, and Raymond Jeanloz, *J. Geophys. Res., 90*, 2057–2059, 1985.

Nakanishi, I., Seismic reflections from the upper mantle discontinuities beneath the Mid-Atlantic Ridge observed by a seismic array in Hokkaido region, Japan, *Geophys. Res. Lett., 13*, 1458–1461, 1986.

Nolet, G., and M.J.R. Wortel, Structure of the upper mantle, in *Encyclopedia of Geophysics*, edited by D. James, Van Nostrand Rheinhold, New York, in press, 1988.

Owens, T.J., G. Zandt, and S.R. Taylor, Seismic evidence for an ancient rift beneath the Cumberland Plateau, Tennessee: A detailed analysis of broadband teleseismic *P* waveforms, *J. Geophys. Res., 89*, 7783–7795, 1984.

Owens, T.J., S.R. Taylor, and G. Zandt, Crustal structure at Regional Seismic Test Network stations determined from inversion of broadband teleseismic *P* waveforms, *Bull. Seismol. Soc. Am., 77*, 631–662, 1987.

Paulssen, H., Upper mantle converted waves beneath the NARS array, *Geophys. Res. Lett., 12*, 709–712, 1985.

Paulssen, H., Lateral heterogeneity of Europe's upper mantle as inferred from modelling of broad-band body waves, *Geophys. J. R. Astron. Soc., 91*, 171–199, 1987.

Paulssen, H., Evidence for small scale structure of the upper mantle, *Ph.D. thesis, University of Utrecht*, pp. 109, 1988.

Phinney, R.A., Structure of the Earth's crust from spectral behavior of long-period body waves, *J. Geophys. Res., 69*, 2997–3017, 1964.

Richards, M.A., and C.H. Wicks, Topography of the '650 km' discontinuity beneath Tonga from *S-P* conversion (abstract), *Eos Trans. AGU, 68*, 1379, 1987.

Richards, P.G., Seismic waves reflected from velocity gradient anomalies within the Earth's upper mantle, *Z. Geophys., 38*, 517–527, 1972.

Richter, F.M., and C.E. Johnson, Stability of a chemically layered mantle, *J. Geophys. Res., 79*, 1635–1639, 1974.

Ringwood, A.E., and T. Irifune, The nature of the 650-km discontinuity: Implications for mantle dynamics, *Nature, 331*, 1988.

Souriau, A., First analyses of broadband records on the GEOSCOPE network: Potential for detailed studies of mantle discontinuities, *Geophys. Res. Lett., 13*, 1011–1014, 1986.

Spakman, W., M.J.R. Wortel, and N.J. Vlaar, The Hellenic subduction zone: a tomographic image and its geodynamic implications, *Geophys. Res. Lett., 13*, 60–63, 1988.

Teng, T.-L., and J.P. Tung, Upper-mantle discontinuity from amplitude data of $P'P'$ and its precursors, *Bull. Seismol. Soc. Am., 63*, 587–597, 1973.

Vinnik, L.P., Detection of waves converted from *P* to *SV* in the mantle, *Phys. Earth Planet. Inter., 15*, 39–45, 1977.

Walck, M.C., The *P*-wave upper mantle structure beneath an active spreading centre: The Gulf of California, *Geophys. J. R. Astron. Soc., 76*, 697–723, 1984.

Whitcomb, J.H., and D.L. Anderson, Reflections of $P'P'$ seismic waves from discontinuities in the mantle, *J. Geophys. Res., 75*, 5713–5728 1970.

H. Paulssen, Department of Theoretical Geophysics, Institute of Earth Sciences, P.O. Box 80.021, 3508 TA Utrecht, The Netherlands.

(Received November 16, 1987;
revised February 17, 1988;
accepted March 6, 1988.)